



Radiation Enhancement with Polyethyleneimine-Coated Gold Nanoparticles Under MV Photons

Süheyla AYTAÇ ARSLAN,¹ Mustafa TÜRK²

¹Department of Radiation Oncology, Ankara Atatürk Research and Training Hospital, Yıldırım Beyazıt University School of Medicine, Ankara-Turkey

²Department of Bio-Engineering, Faculty of Engineering, Kırıkkale University, Kırıkkale-Turkey

OBJECTIVE

Radiotherapy is an essential part of cancer management, and about two-thirds of the patients with cancer receive radiation therapy during their treatment. The healthy structures around the tumor are dose limiting in terms of acute and late toxicity. Radiosensitizers (RSs) can be used to enhance intratumoral dose, thus improving the therapeutic ratio. We aimed to investigate the cytotoxicity on normal and cancer cell lines induced by interaction between MV photon irradiation and polyethyleneimine (PEI)-coated gold nanoparticles (AuNPs).

METHODS

The effects of different concentrations of AuNPs (0.75 µg/ml, 0.5 µg/ml, 0.25 µg/ml, and only medium) and 2 Gy ionizing radiation (IR) were investigated on the L929 fibroblast, DLD-1 colon, and H1299 lung cancer cell lines. Cytoplasmic and nuclear membranes treated with hematoxylin and eosin and double staining were evaluated with light and fluorescence microscopy. Cytotoxicity was determined with the WST-1 method.

RESULTS

All particles were spherical in shape with 60.98 nm in size. Cell surviving ratios without AuNPs were 96.34% in L929, 89.68% in DLD-1, and 76.93% in H1299 for a single 2-Gy radiation. These ratios were 94.2%, 62.58%, and 40.52% for L929 cells; 72.70%, 41.15%, and 26.71% for DLD-1 cells; and 34.72%, 28.27%, and 17.84% for H1299 cells at concentrations of 0.25 µg/ml, 0.5 µg/ml, and 0.75 µg/ml AuNPs, respectively.

CONCLUSION

At increased concentrations, isolated unwanted cytotoxic effects of AuNPs could be observed. Radiosensitizing effect of PEI-coated AuNPs depends on cell type and AuNP concentration.

Keywords: Gold nanoparticle; megavoltage; polyethyleneimine; radiosensitization.

Copyright © 2019, Turkish Society for Radiation Oncology

Introduction

Radiotherapy is an essential part of cancer management, and about 50%–60% of the patients with cancer receive radiotherapy during the treatment of

their illness.[1] The healthy structures around the tumor are dose limiting in terms of acute and late toxicity. Using more precise radiation techniques such as intensity-modulated radiotherapy and applying concurrent chemotherapy and/or hyperthermia as

Received: January 14, 2019

Accepted: March 14, 2019

Online: May 29, 2019

Accessible online at:
www.onkder.org

OPEN ACCESS This work is licensed under a Creative Commons Attribution-NonCommercial 4.0 International License.



Dr. Süheyla AYTAÇ ARSLAN

Ankara Atatürk Araştırma ve Eğitim Hastanesi,

Radyasyon Onkolojisi Bölümü,

Yıldırım Beyazıt Üniversitesi Tıp Fakültesi,

Ankara-Turkey

E-mail: saytac1@yahoo.com

a radiosensitizer (RS) are examples for enhancing intratumoral dose, and they thus improve the therapeutic ratio.[2,3,4]

Nanotechnology is a rapidly developing branch of science. Its use in radiation oncology has three major aspects: 1) facilitate image-guided radiotherapy (IGRT) through mechanisms based on increased uptake of particles by cancer cells similar to positron emission tomography imaging [5]; 2) increased synergistic cytotoxic effects with hyperthermia, chemotherapy, and targeted therapy combinations [6,7,8,9]; and 3) radiation enhancement via radiosensitizing effect.[10]

Gold nanoparticles (AuNPs) are usually various shaped with a size of 1–100 nm and a gold core covered by surface coating.[11] Among the elements with high Z number, AuNPs are the most extensively studied ones because of their relative biocompatibility and ease in size, shape, and surface coating modifications.[4] They are small enough to pass through atypical weakly tumor vasculature so that they can extravagate and accumulate in tumor site much more easily than they do in normal tissues. This is called enhanced permeability and retention effect, and is a key characteristic of AuNPs to introduce into clinical practice. In the bloodstream, they must have sufficient circulating time without interference to the biologic effects that they are exposed to. Upon extravasation from tumor vasculature, they penetrate to the tumor interstitium and distribute homogeneously. Smaller AuNPs are advantageous in achieving more homogeneous intratumoral distribution. Uptake of cells via receptor-mediated endocytosis is dependent on size and shape, and it requires energy.[12] It is known that IR can directly or indirectly damage DNA, and has no selectivity because of the similar mass energy absorption of cancerous and healthy tissues. [13] While cytoplasmic localization of particles can yield radiosensitization, nuclear uptake enables additional DNA damage by low-energy electrons.[14,15] Yet, they must be smaller than 30 nm to allow uptake through the nuclear pore complex. Like most of the drugs, AuNPs are eliminated through kidney (≤ 7 nm) and liver (~ 10 –100 nm). Dedicated particles should be easily excreted by the kidneys with reduced opsonization and clearance by Kupffer cells.[16,17,18]

Over the past decade, the field of AuNP-based radiosensitization has undergone a tremendous growth; this fact is demonstrated by the exponential increase in the number of publications on this topic. Studies regarding AuNP-mediated radiation enhancement have been done from the early 2000s.[19,20] Most of

these studies showed RS effect at superficial kV and less with clinically relevant MV energy levels.[21,22,23] Although there is an ongoing huge preclinical data describing the possible mechanisms behind this radiation enhancement, it is still in infancy. Interaction with matter causes a series of reactions in three phases: physical, chemical, and biological; and recent data show that AuNPs have roles in all these phases of interactions with IR.[4,24,25] It would be plausible to predict that this enhancement can be affected by the modifications of IR parameters (source, energy, dose/fraction); AuNPs (size, shape, surface coating, and functionalization); and the tumor itself such as intrinsic sensitivity, hypoxic fraction, and so on. From bench to bedside use of AuNP as an RS, the optimal concentrations of AuNPs for different types of tumors should be thoroughly examined.[10]

This study aimed to characterize the cytotoxicity on normal fibroblasts (L929), colon (DLD-1), and lung (H1299) cancer cell lines via AuNP-mediated radiation dose enhancement under MV energies.

Materials and Methods

Cell Culture

Colon (DLD-1) and lung (H-1299) cancer cells were obtained from American Type Culture Collection. All cultures were supplemented with 10% fetal bovine serum and 1% penicillin and streptomycin. Cell lines were maintained in monolayers in a tissue culture humidified incubator at 37°C with 5% CO₂/95% air for 24 h and sub-cultured every 3–4 days to maintain exponential growth.

AuNP Synthesis

AuNPs coated with polyethyleneimine (PEI) and 3-aminophenyl boronic acid, which were previously synthesized for another study, were used in our work. [26] AuNPs were added and provided the same concentration of gold nanoparticles in the culture during irradiation.

Irradiation Setup

Megavoltage X-ray (6 MV) irradiations were performed using the Elekta linear accelerator. Petri dishes contain a layer of malignant cells plus about 2 mm of medium and 18 mm air. The prescribed dose was 2 Gy, and SSD was set to 100 cm using a 20×20 cm field. Six centimeters of plexyglass material (water-equivalent) was placed on top of the dish. The dose rate was 3.55 Gy/min.

The gafchromic film was placed under the dishes to evaluate dose homogeneity and to irradiate with a single dose of 2 Gy. After radiation exposure, the dosimetry film demonstrated that the target area was homogeneously exposed to radiation.

Hematoxylin-Eosin Staining

A 20×10^3 cells/well of L929, DLD-1, and H1299 cells were placed in a 48-well plate of 10% fetal bovine serum and 1% penicillin streptomycin containing DMEM and RPMI and incubated with 5% CO₂ at 37°C for 24 h. Afterwards, cells were treated with different amounts of AuNPs (0.25 µg/ml, 0.5 µg/ml, 0.75 µg/ml) and incubated another 24 h and then 2 Gy RT was applied. Alcohol was put into cells in decreasing concentrations (100%, 96%, 80%, 70%, 50%) for 1 min for dehydration. Cell morphology was examined under the light microscope. Experiments were repeated thrice.

Double Staining

Double staining was performed to quantify the number of apoptotic and necrotic cells. The L929, DLD-1, and H1299 cells were placed in 10 ml of PBS solution in a 48-well plate (20×10^3 cells/well). Ribonuclease A inhibits cytoplasmic RNA staining, and propidium iodide stains necrotic and Hoescht 33342 stains apoptotic cells. Cells were subjected to RPMI and DMEM and incubated with 5% CO₂ at 37°C for 24 h. Then three different concentrations (0.75 µg/ml, 0.5 µg/ml, 0.25 µg/ml) of AuNPs were added and incubated for another 24-h repeated thrice. Afterwards, they were washed with PBS (after the incubation, the cells media were discarded) and stained with 70 µl double staining dye for 15 min at dark. Cells were examined with FITC- and DAPI-filtered fluorescent inverted microscope. A 20-fold magnification was used for images.

WST-1 Cytotoxicity Test

Initially cells were plated for 24 h, and then treated with 0.25 µg/ml, 0.50 µg/ml, and 0.75 µg/ml 60.98 nm AuNPs for 24 h. Then cells were washed; and cell media was discarded and incubated in fresh culture medium without 100 µl phenol red. The cells were then exposed to 10 µl WST-1 solution for 4 h, and plates were read using a microplate reader at 440 nm. The cell numbers in the control and AuNP-exposed samples were counted; thus, toxicity of different concentration of AuNPs was analyzed.

Following incubation, the absorbance was measured in a microplate reader at a wavelength of 440 nm to determine the toxicity of the gold particles alone.

In the second phase of the experiment, after 24 h exposure with AuNPs, cells were irradiated with 2 Gy photon beams. After irradiation, AuNP-exposed and unexposed cells (control) were incubated in culture medium for another 24 h, and then viability was tested for the IR and IR+AuNP groups.

Radiation Enhancement Ratio

The radiation enhancement ratio (RER) is defined as the ratio of survival fractions without and with AuNPs for a specific dose that is 2 Gy in this setting. It has the benefit of directly comparing the biologic response caused by the nanoparticles at a specific dose level.

Results

Morphologic Assessment of Cells (H&E staining)

Cells were examined under a light microscope after AuNP and AuNP+IR exposure, and results were presented in Figures 1, 2, 3 and Table 1. Without any exposure, all three types of cells were morphologically normal with a clear cytoplasm-nucleus boundary and placed dispersedly in the medium. After PEI-coated AuNPs exposure, cells morphology was changed according to the amount of AuNPs used.

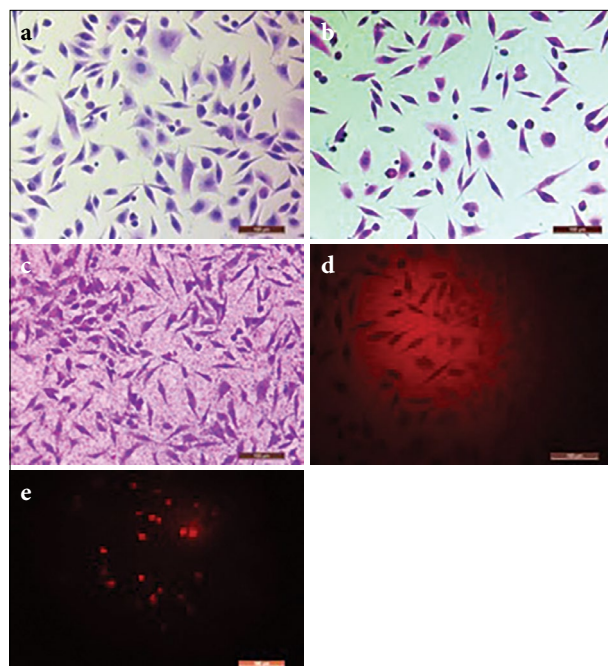


Fig. 1. H&E (a, b, c) and propidium iodide (d, e, f) images of the L929 fibroblasts with light and fluorescein microscopy. (a) only medium, (b) AuNP exposure, (c) AuNP+IR, (d) only medium, (e) AuNP exposure, (f) AuNP+IR.

Cells were aggregated, lost their cytoplasmic membrane integrity, decreased in volume, and detached from the plate. These changes were most abundant in H1299 cells and least in fibroblasts and exacerbated with IR. Cross-linking between positively charged AuNPs with glycosaminoglycan and collagens caused intercellular organic material accumulation leading to cytoplasmic membrane damage. This may result in decreased uptake of nutrients in cancer cells and thus cell death.

Double Staining of Nucleus

The PI-stained necrotic cell ratios and microscopic images are presented in Table 2 and Figures 1, 2, 3. The ratio of necrotic cells with PI-stained nucleus was 1%–

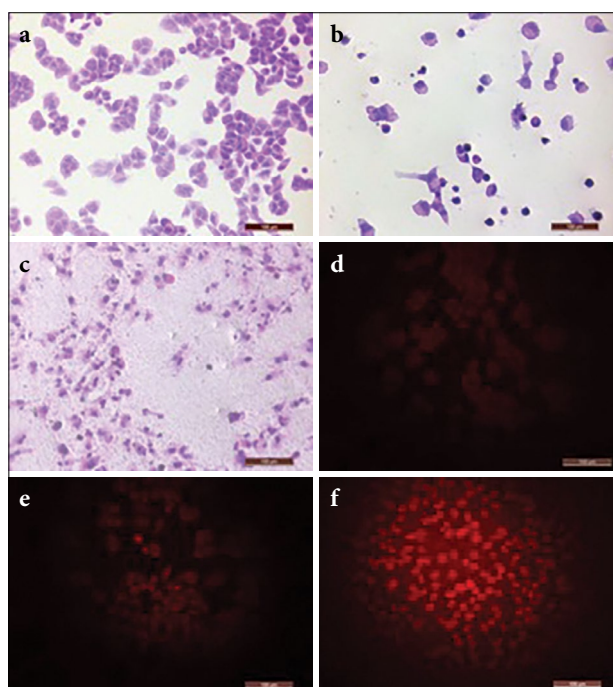


Fig. 2. H&E (a, b, c) and propidium iodide (d, e, f) images of the DLD-1 colon cancer cells with light and fluorescein microscopy. (a) only medium, (b) AuNP exposure, (c) AuNP+IR, (d) only medium, (e) AuNP exposure, (f) AuNP+IR.

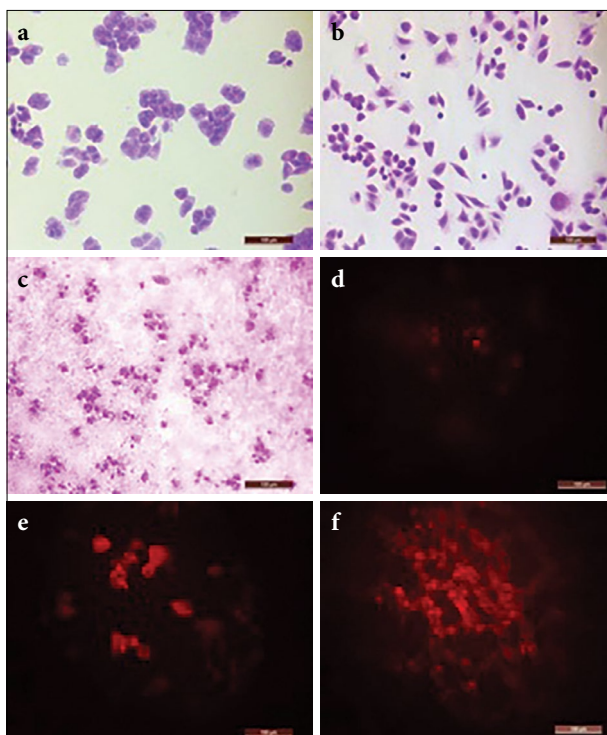


Fig. 3. H&E (a, b, c) and propidium iodide (d, e, f) images of the H1299 lung cancer cells with light and fluorescein microscopy. (a) only medium, (b) AuNP exposure, (c) AuNP+IR, (d) only medium, (e) AuNP exposure, (f) AuNP+IR.

4%, and it increased with increasing AuNP concentrations. The nucleus was mostly intact except H1299 cells with 0.50 and 0.75 µg/ml AuNPs.

Viability

Cell surviving ratios without AuNPs were 96.34% in L929 (Fig. 1), 89.68% in DLD-1 (Fig. 2), and 76.93% in H1299 (Fig. 3) for a single 2-Gy radiation. These ratios were 94.2%, 62.58%, and 40.52% for L929 cells; 84.85%, 78.05%, and 17.84% for DLD-1 cells; 34.72%, 28.27%, and 17.84% for H1299 cells at concentrations of 0.25 µg/ml, 0.5 µg/ml, 0.75 µg/ml AuNPs, respectively. Viability of cells after IR exposure with and without AuNPs is represented in Tables 3 and 4.

Table 1 H&E staining results of damaged cell (%)

	Medium	Medium+IR	0.25 AuNP+IR	0.50 AuNP+IR	0.75 AuNP+IR
L929	0	3	5	28	42
DLD-1	0	12	24	51	68
H1299	0	22	48	67	81

Abb: IR, Ionizing radiation; AuNP: Gold nanoparticle.

Table 2 PI staining results of necrotic cells (%)

	Medium	Medium+IR	0.25 AuNP+IR	0.50 AuNP+IR	0.75 AuNP+IR
L929	2	5	6	32	53
DLD-1	3	14	27	63	79
H1299	4	26	64	72	84

Abb: IR, Ionizing radiation; AuNP: Gold nanoparticle.

Table 3 Cell viability ratios with and without AuNP (\pm SD)

	0.25 μ g/ml	0.50 μ g/ml	0.75 μ g/ml
L929	104.39 \pm 0.04	84.41 \pm 0.06	52.90 \pm 0.00
DLD-1	84.85 \pm 0.01	78.05 \pm 0.01	47.93 \pm 0.02
H1299	69.40 \pm 0.00	45.78 \pm 0.02	38.10 \pm 0.02

AuNP: Gold nanoparticle; SD: Standard deviation.

Radiation Enhancement Ratio

Radiation enhancement ratio (RER_{2Gy}) for DLD-1 was 1.23 and for H1299 was 2.21 with 0.25 μ g/ml concentrations of AuNPs.

Discussion

Gold has long been used in the therapeutic and diagnostic medicine because it is considered as an inert, nontoxic, biocompatible metal. It has been widely studied in current medical and biological research in nanoscale level, and many researches have been done to investigate the possible role of them in the clinical setting.[10,27,28] Naked AuNPs are significantly toxic both in vitro and in vivo, and appropriate coating may lessen these detrimental effects. Surface chemistry is also an important key parameter.[9] Highly positive NPs bind to negatively charged DNA causing damage to it. Amine groups also enable specific targeting of cells, for example, drugs.[29,30]

In this study, we used 60.98 nm spherical AuNPs coated with cationic charged PEI and 0.25 μ g/ml AuNPs concentration considered to be safe so that at least 69% viability observed cancerous cell lines and fi-

broblast continued to proliferate. The toxic effect due to AuNPs showed a significant difference between normal and cancerous cells at low concentrations, but this difference gradually diminished with increasing concentrations. The level of toxicity was also different for different tumor types; H1299 appears to be the most vulnerable group. In a study by Coulter et al., they found that AuNP uptake was preferentially observed in tumor cells, and cytotoxicity was low, so that particle concentration causing 50% of growth inhibition in cell culture defined as IC₅₀ for normal cells were 14 times higher than tumor cells.[13] They also showed that intracellular accumulation of gold occurs in concentration and time-dependent manner. Toxic effects of nanoparticles seen more frequently on tumor cells suggest the enhanced permeation and retention effect in vivo described by Maeda et al.[31]

Formerly, radiosensitization has mainly been attributed to physical dose enhancement occurring at kilovoltage (kV) photon energies by means of photoelectric absorption of gold as a high Z material. However, data about different mechanisms of radiobiological effects regarding radiosensitization are growing [4], and experimental studies using clinically relevant MV energies showed significant dose enhancements in vitro and in vivo suggesting other possible mechanisms of biological action, for example, oxidative stress, cell cycle distribution, and DNA repair inhibition rather than physical enhancement.[32] With the same concentration, we studied the radiation enhancement effect difference in different cancer cells. In this study, 0.25 μ g/ml dose concentration of nanoparticle was found to be safer, and an RER of 1.23 and 2.21 were found for

Table 4 Cell viability ratios with and without AuNPs after 2 Gy radiation exposure (\pm SD)

	Only Medium	Only IR	0.25 μ g/ml+IR	0.5 μ g/ml+IR	0.75 μ g/ml+IR
L929	100	96.34 \pm 0.76	94.26 \pm 0.02	62.58 \pm 0.01	40.52 \pm 0.01
DLD-1	100	89.68 \pm 0.54	72.70 \pm 0.01	41.15 \pm 0.01	26.71 \pm 0.02
H1299	100	76.93 \pm 2.48	34.72 \pm 0.00	28.27 \pm 0.02	17.84 \pm 0.00

Abb: IR, Ionizing radiation; SD: Standard deviation.

DLD-1 and H1299 cells, respectively. Our observation was consistent with the results of previous studies that radiation sensitization may change with different cell types. In addition, Her et al. evaluated the radiosensitization effects of polyethylene glycol-stabilized AuNPs (PEG-AuNPs) in two human triple-negative cell lines (MDA-MB-231 and MDA-MB-436), and they found that PEG-AuNPs sensitized both cell lines to radiation, achieving dose enhancement factors of 1.26 and 1.15, respectively.[33]

The surface coating is an important parameter to control particle stability solubility and biocompatibility.[34,35] It also enables targeting of antibodies, drugs, and radionuclides. Citrate, polyethylene glycol, and thiol are frequently used coatings. They also led to necrosis by enhanced ROS production. PEI, which is used as a coating in this study, is a cationic polymer that binds to the anionic cell membrane phospholipids and enables uptake.[36] It can be used as a gene delivery vehicle [37], a contrast agent for imaging [38,39], and a biosensor for glutamate detection.[40]

Chithrani et al. evaluated the size and shape dependence of AuNPs' uptake into mammalian cells, and observed the highest uptake and radiosensitization with approximately 50 nm compared to the 14 nm and 70 nm.[41] They were also the first who observed relatively decreased but still significant radiosensitization at MV energies.[42] They showed that HeLa cells treated with 50 nm citrate-AuNPs increased the number of γ -H2AX and 53BP1 foci at 4 and 24 h post-irradiation at both 220 kVp and 6 MV energies that were indicative of delayed DNA repair, a key mode of radiosensitization.

Wang et al. reported the radiosensitization effect of glucose-capped AuNPs with different sizes (16 nm and 49 nm) on triple-negative breast cancer cells in the presence of MV energy. They showed increased RS effect with 49 nm AuNPs with an SER of 1.86 compared to 16 nm AuNPs with an SER of 1.49. Moreover, they demonstrated that the rate of the cells arrested in G2/M phase were increased with AuNPs' exposure, more with 49 nm AuNPs, a possible mechanism for enhanced radiation sensitization effect because G2/M phase is the most radiosensitive phase of the cell cycle. [43] We found an RER of 1.23 and 2.21 for colon and lung cancer cells with similar size but different coating AuNPs. Not only particle size but shape, surface coating, concentration, and cell type may change radiation enhancement. To date, because different approaches, for example, SER, DMRX%, REF is used to quantify NP radiation enhancement effect; it is challenging to

interpret the results even with identical nanoparticles and cell type.

There are certain limitations of the study. First, although staining of cells showed us cell membrane, cytoplasm, and nuclear damage, we were not able to determine the intracellular distribution of AuNPs, in terms of uptake and localization that can affect both the isolated toxicity of AuNPs and radio sensitization. Defining the underlying mechanism for RS effect is also critical for possible further clinical application.

AuNP-related cytotoxicity was observed not only in cancerous cells but also in noncancerous fibroblasts. This toxic effect is more pronounced at increasing concentrations that can limit the use of AuNP. This study also suggests that lower concentration of AuNPs acting only on cancer cells can be used as RSs and are cell-type dependent.

Peer-review: Externally peer-reviewed.

Conflict of Interest: No conflict of interest.

Financial Support: No financial support.

Authorship contributions: Concept – S.A.A., M.T.; Design – S.A.A., M.T.; Supervision – S.A.A., M.T.; Materials – S.A.A., M.T.; Data collection &/or processing – S.A.A., M.T.; Analysis and/or interpretation – S.A.A., M.T.; Literature search – S.A.A.; Writing – S.A.A.; Critical review – S.A.A.

References

1. Delaney G, Jacob S, Featherstone C, Barton M. The role of radiotherapy in cancer treatment: estimating optimal utilization from a review of evidence-based clinical guidelines. *Cancer* 2005;104(6):1129–37.
2. Chen AM, Yang CC, Marsano J, Liu T, Purdy JA. Intensity-modulated radiotherapy for nasopharyngeal carcinoma: improvement of the therapeutic ratio with helical tomotherapy vs segmental multileaf collimator-based techniques. *Br J Radiol* 2012;85(1016):e537–43.
3. Arslan SA, Ozdemir N, Sendur MA, Eren T, Ozturk HF, Aral IP, et al. Hyperthermia and radiotherapy combination for locoregional recurrences of breast cancer: a review. *Breast Cancer Management* 2017;6(4):117–26.
4. Her S, Jaffray DA, Allen C. Gold nanoparticles for applications in cancer radiotherapy: Mechanisms and recent advancements. *Adv Drug Deliv Rev* 2017;109:84–101.
5. AlZaki A, Joh D, Cheng Z, De Barros AL, Kao G, Dorsey J, et al. Gold-loaded polymeric micelles for computed tomography-guided radiation therapy treatment and radiosensitization. *ACS Nano* 2014;8(1):104–12.
6. Diagaradjane P, Shetty A, Wang JC, Elliott AM, Schwartz J, Shentu S, et al. Modulation of in vivo tu-

- mor radiation response via gold nanoshell-mediated vascular-focused hyperthermia: characterizing an integrated antihypoxic and localized vascular disrupting targeting strategy. *Nano Lett* 2008;8:1492–500.
7. Setua S, Ouberaï M, Piccirillo SG, Watts C, Welland M. Cisplatin-tethered gold nanospheres for multimodal chemo-radiotherapy of glioblastoma. *Nanoscale* 2014;6(18):10865–73.
 8. Bonner JA, Lawrence TS. Doxorubicin decreases the repair of radiation-induced DNA damage. *Int J Radiat Biol* 1990;57:55–64.
 9. Hainfeld JF, O'Connor MJ, Dilmanian FA, Slatkin DN, Adams DJ, Smilowitz HM. Micro-CT enables microlocalisation and quantification of Her2-targeted gold nanoparticles within tumour regions. *Br J Radiol* 2011;84(1002):526–33.
 10. Wang AZ, Tepper JE. Nanotechnology in radiation oncology. *J Clin Oncol* 2014;32(26):2879–85.
 11. Grzelczak M, Pérez-Juste J, Mulvaney P, Liz-Marzán LM. Shape control in gold nanoparticle synthesis. *Chem Soc Rev* 2008;37(9):1783–91.
 12. Huo S, Ma H, Huang K, Liu J, Wei T, Jin S, et al. Superior penetration and retention behavior of 50 nm gold nanoparticles in tumors. *Cancer Res* 2013;73(1):319–30.
 13. Coulter JA, Jain S, Butterworth KT, Taggart LE, Dickson GR, McMahon SJ, et al. Cell type-dependent uptake, localization, and cytotoxicity of 1.9 nm gold nanoparticles. *Int J Nanomedicine* 2012;7:2673–85.
 14. Xiao F, Zheng Y, Cloutier P, He Y, Hunting D, Sanche L. On the role of low-energy electrons in the radiosensitization of DNA by gold nanoparticles. *Nanotechnology* 2011;22(46):465101.
 15. McMahon SJ, Hyland WB, Muir MF, Coulter JA, Jain S, Butterworth KT, et al. Biological consequences of nanoscale energy deposition near irradiated heavy atomnanoparticles. *Sci Rep* 2011;1:18.
 16. Fraga S, Brandão A, Soares ME, Morais T, Duarte JA, Pereira L, et al. Short- and long-term distribution and toxicity of gold nanoparticles in the rat after a single-dose intravenous administration. *Nanomedicine* 2014;10(8):1757–66.
 17. Sadauskas E, Danscher G, Stoltenberg M, Vogel U, Larsen A, Wallin H. Protracted elimination of gold nanoparticles from mouse liver. *Nanomedicine* 2009;5(2):162–9.
 18. Hwang JH, Kim SJ, Kim YH, Noh JR, Gang GT, Chung BH, et al. Susceptibility to gold nanoparticle-induced hepatotoxicity is enhanced in a mouse model of nonalcoholic steatohepatitis. *Toxicology* 2012;294(1):27–35.
 19. Hainfeld JF, Slatkin DN, Smilowitz HM. The use of gold nanoparticles to enhance radiotherapy in mice. *Phys Med Biol* 2004;49(18):N309–15.
 20. Mesa AV, Norman A, Solberg TD, Demarco JJ, Smathers JB. Dose distributions using kilovoltage x-rays and dose enhancement from iodine contrast agents. *Phys Med Biol* 1999;44(8):1955–68.
 21. Khoshgard K, Hashemi B, Arbabi A, Rasaei MJ, Soleimani M. Radiosensitization effect of folate-conjugated gold nanoparticles on HeLa cancer cells under orthovoltage superficial radiotherapy techniques. *Phys Med Biol* 2014;59(9):2249–63.
 22. Lin Y, McMahon SJ, Scarpelli M, Paganetti H, Schuemann J. Comparing gold nano-particle enhanced radiotherapy with protons, megavoltage photons and kilovoltage photons: a Monte Carlo simulation. *Phys Med Biol* 2014;59(24):7675–89.
 23. Lin Y, McMahon SJ, Paganetti H, Schuemann J. Biological modeling of gold nanoparticle enhanced radiotherapy for proton therapy. *Phys Med Biol* 2015;60(10):4149–68.
 24. Misawa M, Takahashi J. Generation of reactive oxygen species induced by gold nanoparticles under x-ray and UV irradiations. *Nanomedicine* 2011;7(5):604–14.
 25. Cheng NN, Starkewolf Z, Davidson RA, Sharmah A, Lee C, Lien J, Guo T. Chemical enhancement by nanomaterials under X-ray irradiation. *J Am Chem Soc* 2012;134(4):1950–3.
 26. Çiftçi H, Alver E, Çelik F, Metin A, Tamer U. Non-enzymatic sensing of glucose using a glassy carbon electrode modified with gold nanoparticles coated with polyethyleneimine and 3-aminophenylboronic acid. *Microchim Acta* 2016;183:1479–86.
 27. Zheng Y, Hunting DJ, Ayotte P, Sanche L. Radiosensitization of DNA by gold nanoparticles irradiated with high-energy electrons. *Radiat Res* 2008;169(1):19–27.
 28. Wolfe T, Chatterjee D, Lee J, Grant JD, Bhattarai S, Tailor R, et al. Targeted gold nanoparticles enhance sensitization of prostate tumors to megavoltage radiation therapy in vivo. *Nanomedicine* 2015;11(5):1277–83.
 29. Zheng Y, Sanche L. Gold nanoparticles enhance DNA damage induced by anti-cancer drugs and radiation. *Radiat Res* 2009;172(1):114–9.
 30. Rathinaraj P, Lee K, Park SY, Kang IK. Targeted images of KB cells using folate-conjugated gold nanoparticles. *Nanoscale Res Lett* 2015;10:5.
 31. Maeda H, Nakamura H, Fang J. The EPR effect for macromolecular drug delivery to solid tumors: Improvement of tumor uptake, lowering of systemic toxicity, and distinct tumor imaging in vivo. *Adv Drug Deliv Rev* 2013;65(1):71–9.
 32. Schuemann J, Berbeco R, Chithrani DB, Cho SH, Kumar R, McMahon SJ, et al. Roadmap to Clinical Use of Gold Nanoparticles for Radiation Sensitization. *Int J Radiat Oncol Biol Phys* 2016;94(1):189–205.
 33. Her S, Cui L, Bristow RG, Allen C. Dual Action Enhancement of Gold Nanoparticle Radiosensitization by Pentamidine in Triple Negative Breast Cancer. *Radiat Res* 2016;185(5):549–62.

34. Kobayashi K, Wei JJ, Lida R, Ijiro K, Niikura K. Surface Engineering of Nanoparticles for Therapeutic Applications. *Polym J* 2014;46:460–8.
35. Kumari A, Yadav SK. Cellular interactions of therapeutically delivered nanoparticles. *Expert Opin Drug Deliv* 2011;8(2):141–51.
36. Godbey WT, Wu KK, Mikos AG. Poly(ethyleneimine) and its role in gene delivery. *J Control Release* 1999;60(2-3):149–60.
37. Kichler A, Leborgne C, Coeytaux E, Danos O. Polyethylenimine-mediated gene delivery: a mechanistic study. *J Gene Med* 2001;3(2):135–44.
38. Zhang Y, Wen S, Zhao L, Li D, Liu C, Jiang W, et al. Ultrasound-stable polyethyleneimine-stabilized gold nanoparticles modified with polyethylene glycol for blood pool, lymph node and tumor CT imaging. *Nanoscale* 2016;8(10):5567–77.
39. Luo X, Peng X, Hou J, Wu S, Shen J, Wang L. Folic acid-functionalized polyethylenimine superparamagnetic iron oxide nanoparticles as theranostic agents for magnetic resonance imaging and PD-L1 siRNA delivery for gastric cancer. *Int J Nanomedicine* 2017;12:5331–5343.
40. Hamdan SK, Mohd Zain A. In vivo Electrochemical Biosensor for Brain Glutamate Detection: A Mini Review. *Malays J Med Sci* 2014;21:12–26.
41. Chithrani BD, Ghazani AA, Chan WC. Determining the size and shape dependence of gold nanoparticle uptake into mammalian cells. *Nano Lett* 2006;6(4):662–8.
42. Chithrani DB, Jelveh S, Jalali F, van Prooijen M, Allen C, Bristow RG, et al. Gold nanoparticles as radiation sensitizers in cancer therapy. *Radiat Res* 2010;173(6):719–28.
43. Wang C, Jiang Y, Li X, Hu L. Thioglucose-bound gold nanoparticles increase the radiosensitivity of a triple-negative breast cancer cell line (MDA-MB-231). *Breast Cancer* 2015;22(4):413–20.